JOURNAL OF MECHANICS OF CONTINUA AND MATHEMATICAL SCIENCES
www.journalimcms.org

ISSN (Online) : 2454 -7190 Vol.-17, No.-1, January (2022) pp 54-64 ISSN (Print) 0973-8975

HYDROTHERMAL BEHAVIOR OF FLUID FLOW AND HEAT TRANSFER THROUGH A BENDING SQUARE CHANNEL

Selim Hussen[1], Ratan Kumar Chanda[2], Rabindra Nath Mondal[3]

[1]Department of Mathematics, Hamdard University Bangladesh, Munshiganj-1510, Bangladesh

[2,3] Department of Mathematics, Jagannath University, Dhaka-1100, Bangladesh

Corresponding author: **Rabindra Nath Mondal**

rnmondal71@yahoo.com

https://doi.org/10.26782/jmcms.2022.01.00004

(Received: November 3, 2021; Accepted: January 2, 2022)

Abstract.

The numerous applications in medical fields as well as in industrial areas have drawn substantial attention from researchers to study the fluid flow and heat transfer (HT) through a bent duct. The present paper demonstrates a spectral-based numerical study of 2D flow in a bent square geometry for various curvature ratios. The numerical calculation has been conducted over Dn, $0 < Dn \leq 5000$ *and the curvature ranges from 0.001 to 0.5. The horizontal walls are thermally different where the bottom wall is heated while the ceiling wall is cooled, the vertical walls being thermally insulated. After an extensive investigation, we found two branching structures of the solution, each consisting of two branches with 2- to 8-vortex solutions for small and medium curvatures while three branches of solution structure for large curvatures. The instability of the flow is then calculated by performing a time-evolution (TEv) analysis and by sketching the phase-space (PS) of the solutions. This study also demonstrates that the HT is significantly boosted with the effect of secondary flows (SF) and the increasing secondary vortices boost heat transfer more effectively than other physically realizable solutions.*

Keywords: Heat transfer, 2D flow, Time-Evolution (TEv), Phase-Space (PS)

I. Introduction

Fluid flows through ducts and channels have been an essential interest of plentiful investigators due to the numerous applications in engineering fields and in many industrial technologies including refrigeration, heat exchanger, rocket engines, combustion engine, cooling, and air condition system, turbines

of gas, etc. Centrifugal forces due to channel curvature attribute twisted flow known as SF. Because of Coriolis and centrifugal forces, two types of secondary forces are produced and the influence of these two forces generates intricate shape of the SF and the axial flow (AF) and appear an additional couple of secondary vortices at the concave wall, which are specially recognized as *Dean Vortices* [XIV]. Since then, several numbers of researchers have investigated this flow with theoretical and experimental at different times. We can refer here to some articles; Berger *et al*. [XI], Nandakumar and Masliyah [III], Ito [II]. Yanase *et al*. [XIII] have studied the solution structure of steady solution (SS) through a curved rectangular duct (CRD) of large Ars. They obtained five branches by investigating the linear stability of the branches. After that, Mondal *et al*. [X] have studied the solution structure of the SS and they have shown the connectivity between SS and unsteady solution (US). Mondal *et al*. [IX] had studied the USs where the flow through a CRD of large Ars. Rotational effects for unsteady flows on solution structures through a CRD have been discussed very recently by Islam *et al*. [VI]. Dolon *et al*. [XII] have analyzed the study on solution structure along with the TEv for strong curvatures. Norouzi *et al*. [V] have investigated the creeping flow and inertial for second-order fluid through the CSD by using FDM. Yamamoto *et al*. [IV] conducted an experimental study for investigating the characteristics of the Dean flow using the visualization method for the CSD. Chanda et al. [I] studied the numerical investigation through a CRD for both positive and negative rotation cases and discussed the HT for CRD flow. In this paper, we studied the hydrothermal behavior of the flow of fluids and the transfer of heat through a bending square channel for various curvatures.

II. Model Set-Up

We assumed 2D, incompressible, and viscous fluid flows through a CSD. Fig. 1 demonstrated the cross-sectional view of the present system. The bottom and top walls are considered to be heating and cooling respectively. The fluid passes through the duct's center lines in the axial direction.

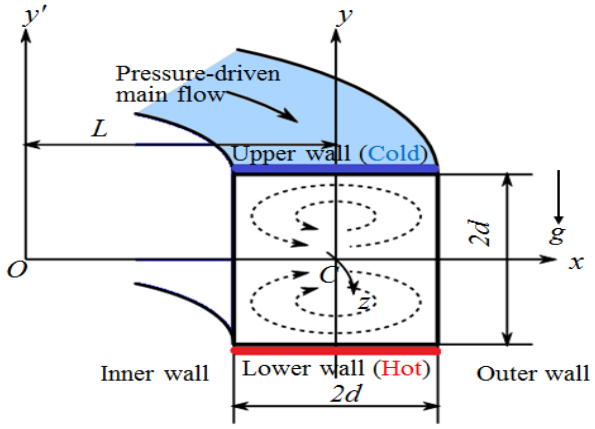

Fig 1. Cross-sectional view of the working system

Because of the uniform fluid flow in z -direction, we introduce the stream function, ψ in the *x*-direction and *y*-direction as

$$u = \frac{1}{1+\delta x}\frac{\partial \psi}{\partial y} \quad \text{and} \, v = -\frac{1}{1+\delta x}\frac{\partial \psi}{\partial x} \tag{1}$$

Therefore, the dimensionless basic equation for the w, ψ and T can be expressed as follows

$$(1+\delta x)\frac{\partial w}{\partial t} = Dn + (1+\delta x)\Delta_2 w - \frac{\partial(w,\psi)}{\partial(x,y)} - \frac{\delta^2 w}{1+\delta x} - \frac{\delta}{(1+\delta x)}\frac{\partial \psi}{\partial y}w + \delta\frac{\partial w}{\partial x} \tag{2}$$

$$\left(\Delta_2 - \frac{\delta}{1+\delta x}\frac{\partial}{\partial x}\right)\frac{\partial \psi}{\partial t} = -\frac{1}{(1+\delta x)}\frac{\partial(\Delta_2\psi,\psi)}{\partial(x,y)} + \frac{\delta}{(1+\delta x)^2}\left[\frac{\partial \psi}{\partial y}\left(2\Delta_2\psi\right) - \frac{3\delta}{1+\delta x}\frac{\partial \psi}{\partial x} + \frac{\partial^2\psi}{\partial x^2}\frac{\partial \psi}{\partial x}\frac{\partial^2\psi}{\partial x \partial y}\right]$$
$$+\frac{\delta}{(1+\delta x)^2}\times\left[3\delta\frac{\partial^2\psi}{\partial x^2} - \frac{3\delta^2}{1+\delta x}\frac{\partial \psi}{\partial x}\right] - \frac{2\delta}{1+\delta x}\frac{\partial}{\partial x}\Delta_2\psi + w\frac{\partial w}{\partial y} + \Delta_2{}^2\psi - Gr(1+\delta x)\frac{\partial T}{\partial x} \tag{3}$$

and

$$\frac{\partial T}{\partial t} = \frac{1}{\Pr}\left(\Delta_2 T + \frac{\delta}{1+\delta x}\frac{\partial T}{\partial x}\right) - \frac{1}{(1+\delta x)}\frac{\partial(T,\psi)}{\partial(x,y)} \tag{4}$$

The dimensionless parameters *Dn* , *Gr* and Pr are defined as

$$Dn = \frac{Gd^3}{\mu\upsilon}\sqrt{\frac{2d}{L}}\,, \; Gr = \frac{\beta g \Delta T d^3}{\upsilon^2}, \Pr = \frac{\upsilon}{\kappa} \tag{5}$$

Boundary Conditions for the *w* and ψ are to be taken as

$$w(\pm 1, y) = w(x, \pm 1) = \psi(\pm 1, y) = \psi(x, \pm 1) = \frac{\partial \psi}{\partial x}(\pm 1, y) = \frac{\partial \psi}{\partial y}(x, \pm 1) = 0 \tag{6}$$

The boundary condition for *T:*

$$T(1, y) = 1, \quad T(-1, y) = -1, \; T(x, \pm 1) = x \tag{7}$$

III. Resistance Coefficient

The resistance coefficient λ, alternative name *hydraulic resistance coefficient*, is defined by the following formula

$$\frac{p_1^* - p_{21}^*}{\Delta_{z^*}} = \frac{\lambda}{d_h^*}\frac{1}{2}\rho\left\langle \omega^* \right\rangle^2 \tag{8}$$

Here, d_h^* represents hydraulic diameters. The velocities through the main axial $\left\langle \omega^* \right\rangle$ are calculated using the following formula

$$\langle \omega^* \rangle = \frac{\nu}{4\sqrt{2\delta d}}\int_{-1}^{1} dx \int_{-1}^{1} \omega(x, y, t)\, dy \tag{9}$$

λ is related to the mean non-dimensional axial velocity $\langle\omega\rangle$ as

$$\lambda = \frac{4\sqrt{2\delta}\,Dn}{\langle\omega\rangle^2} \tag{10}$$

IV. Results and discussion

IV.i. Branching structure

Firstly, we have investigated the solution structure for SSs for $\delta = 0.001,\ 0.1$ and 0.5. After vast investigation, we obtained asymmetric two branches of SSs for each of $\delta = 0.001$ and $\delta = 0.1$ while three branches of SSs for $\delta = 0.5$ over the ranges $0 < Dn \le 5000$. The solution structure of SSs has been visualized in Fig. 2(a) for $\delta = 0.001$, 0.1 and 0.5 for $0 < Dn \le 5000$. The branches are named as the *first branch*, *second branch*, and *third branch* respectively for each curvature. For clear visualization, Fig. 2(a) is presented by enlarging in Fig. 2(b) for all three curvatures. Thereafter, we have obtained the streamlines and isotherms of SFs which are depicted in Fig. 3 for various *Dn* and curvatures. We found no bifurcating relation among three branches.

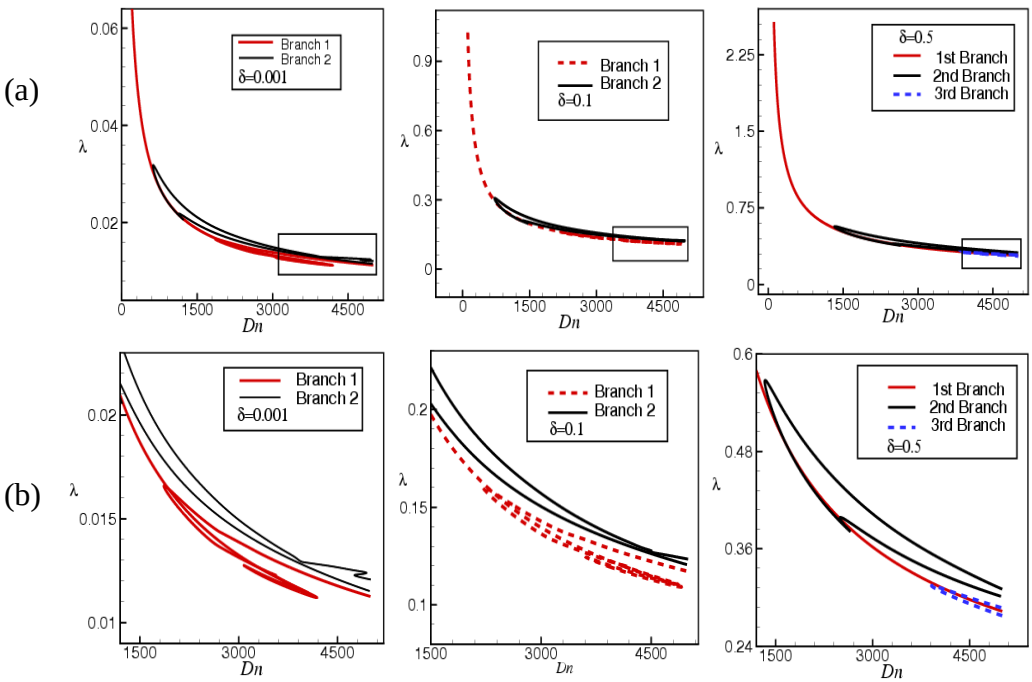

Fig 2. (a) Branching structures for SSs (b) Enlargements of Figure 2(a); (i) $\delta = 0.001$, (ii) $\delta = 0.1$ and (iii) $\delta = 0.5$.

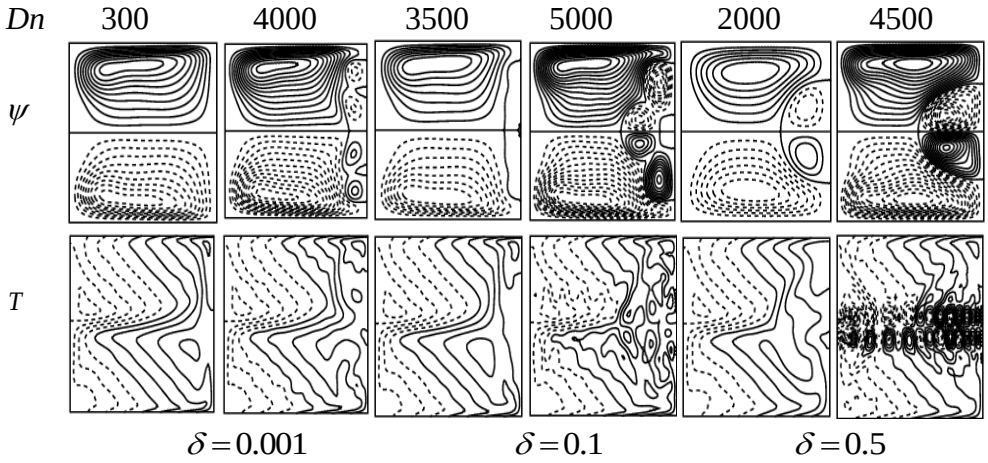

Fig 3. Patterns of the SF (top) and Isotherms (bottom) for different *Dn* and different curvatures δ = 0.001, 0.1, and 0.5.

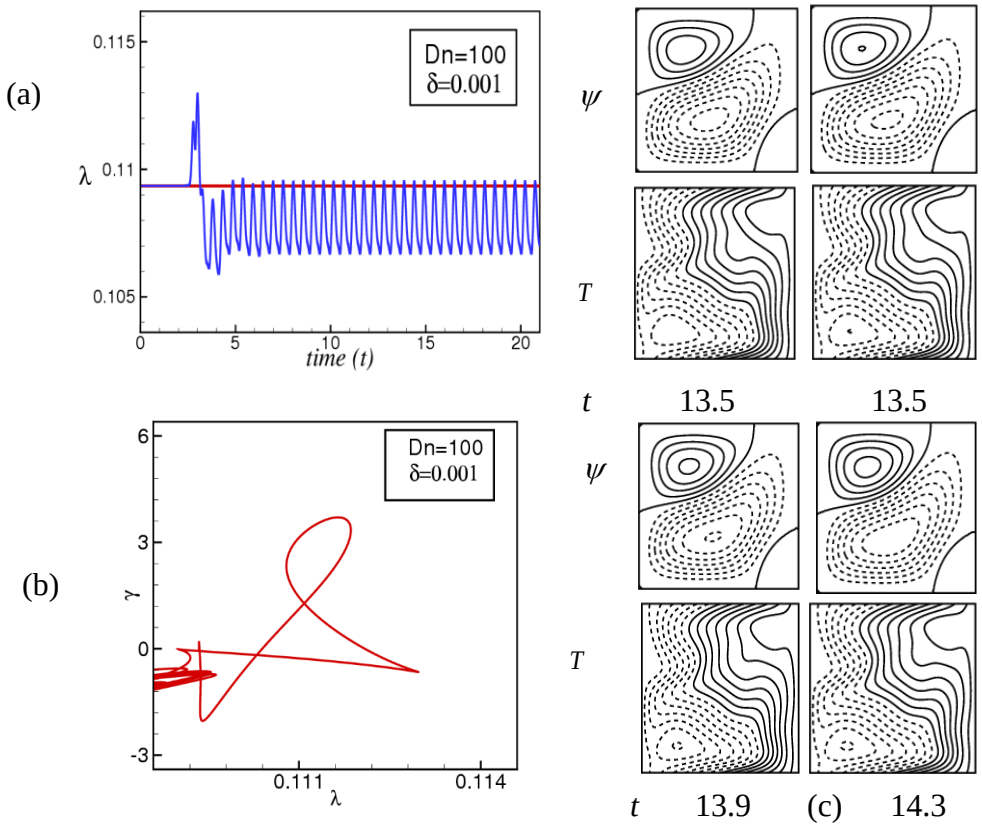

Fig. 4. (a) Time progress, (b) PS and (c) Patterns of the SF (top) and isotherms (bottom) for $Dn = 100$ and $\delta = 0.001$

IV.ii. Unsteady solutions.

We have obtained the time-dependent solutions for $Dn = 100$, $\delta = 0.001$ as depicted in Fig. 4(a). It is observed that the unsteady flow is multi-period in nature with 2- and 3- vortex solutions (Fig. 4(c)). This multi-periodic oscillation has been properly justified by sketching PS diagram in $\lambda - \gamma$ plane as presented in Fig. 4(b). The oscillation of multi-periodicity has turned into steady states $Dn = 500$ with 2- vortex solution as shown in Figs. 5 (a, b) and the steady-state flows are observed to be continued till $Dn = 3500$. Further, an increase of *Dn* numbers at $Dn = 4000$ then we observed that the flow oscillation is irregular with 4- vortex solution (see Figs. 6(a, c)). For good justification, we draw PS of the unsteady solution (US) as exhibited in Fig.6(b) where the orbits cross irregular patterns.

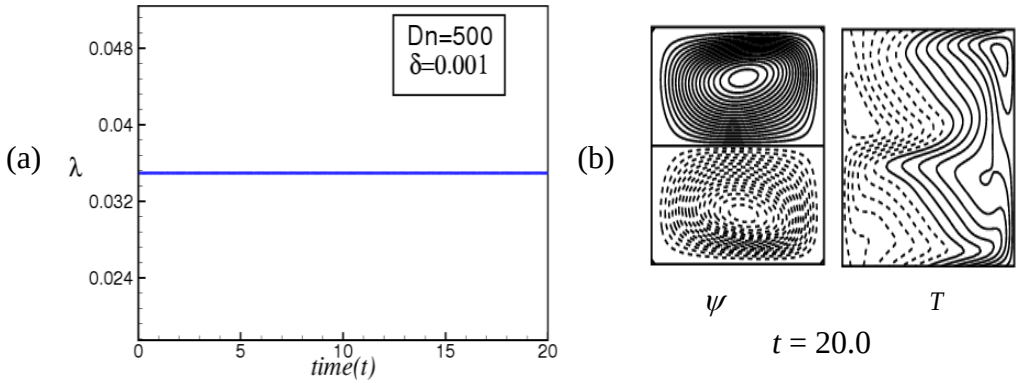

Figure 5. (a) Time progress (b) Patterns of the SF (top) and isotherms (bottom) for $Dn = 500$ and $\delta = 0.001$

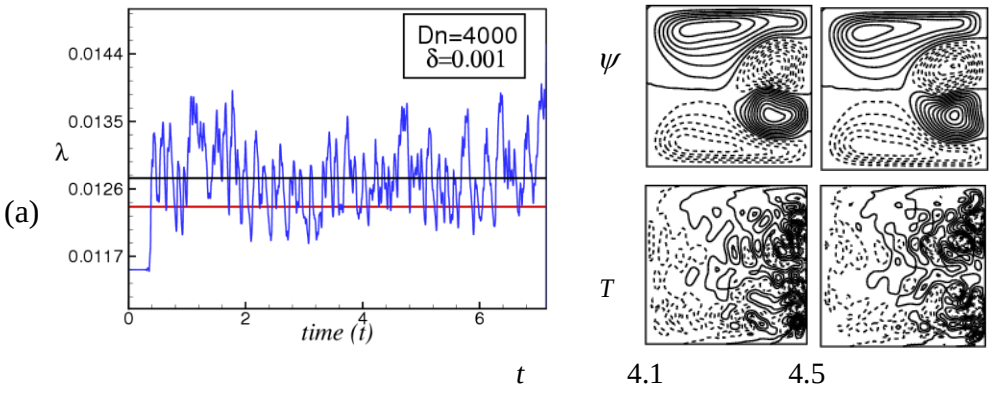

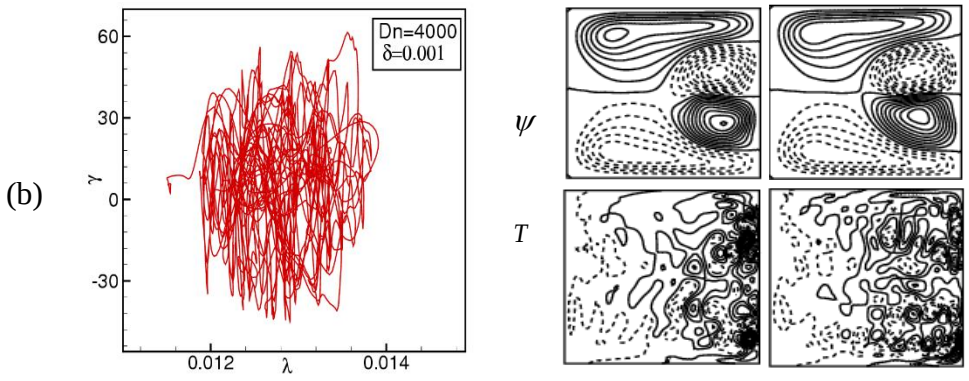

Fig 6. (a) Time progress, (b) PS and (c) Patterns for SF (top) and the isotherms (bottom) for $Dn = 4000$ and $\delta = 0.001$

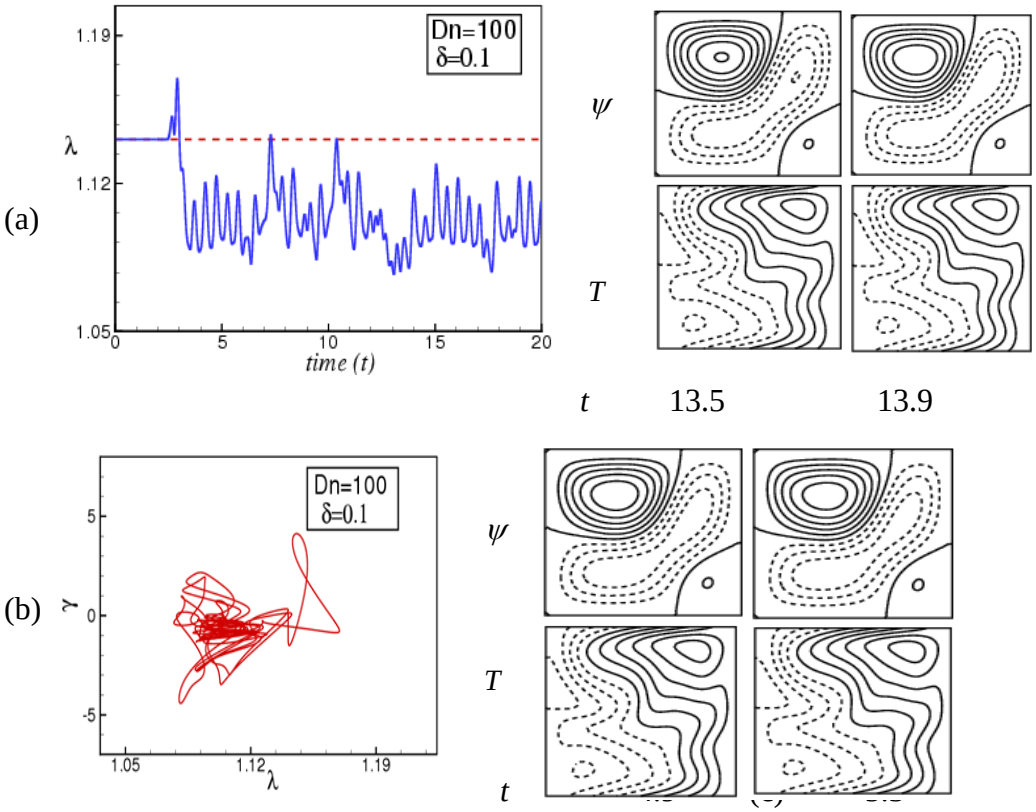

Fig 7. (a) Time progress, (b) PS and (c) Patterns of the SF (top) and the Isotherms (bottom) for $Dn = 100$ and $\delta = 0.1$.

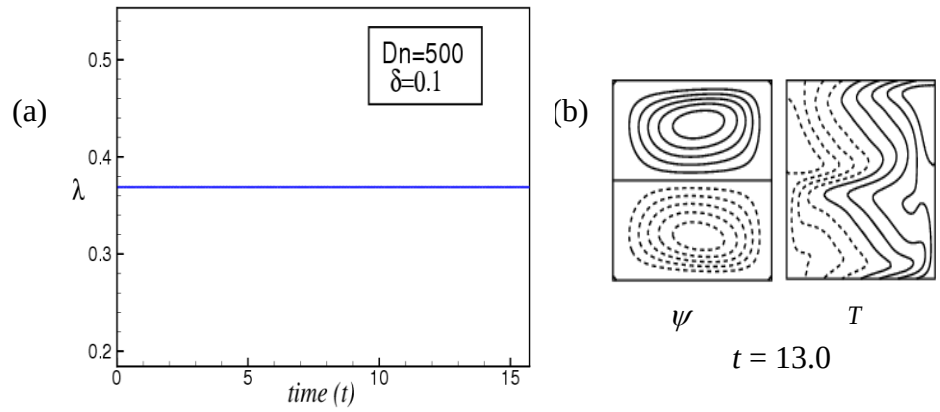

Fig8. (a) Time progress, (b) Patterns of the SF (top) and the isotherms (bottom) for $Dn = 500$ and $\delta = 0.1$.

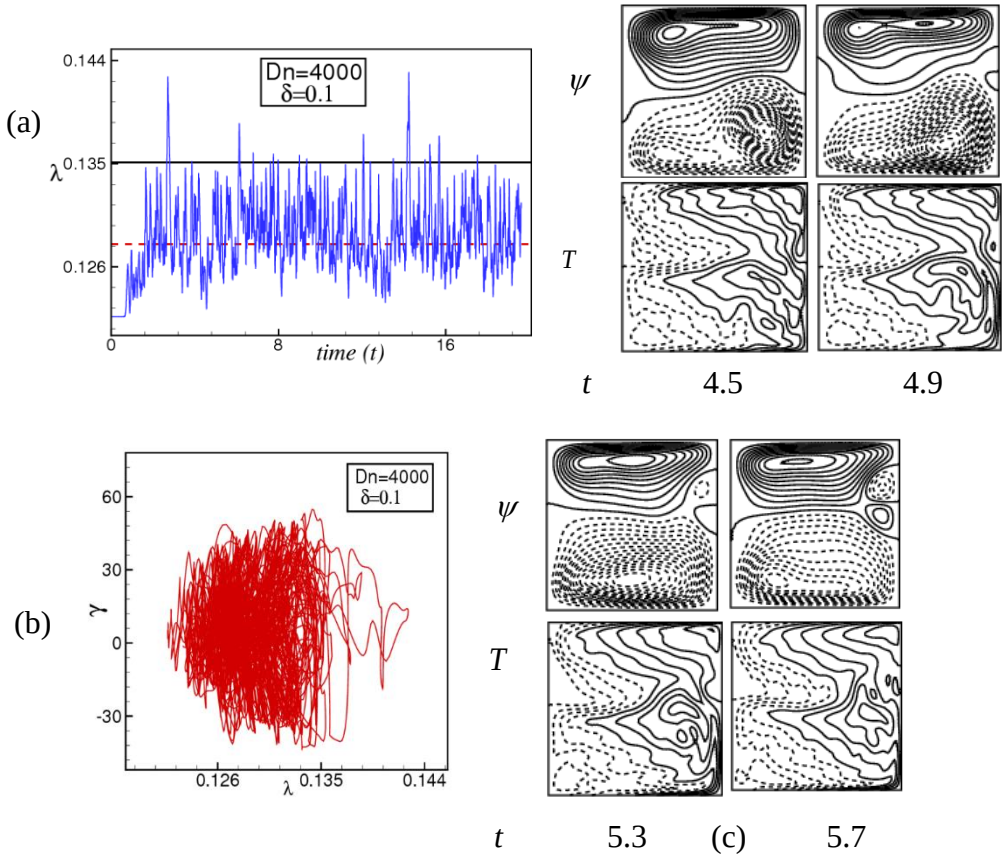

Fig 9. (a) Time progress, (b) PS and (c) Patterns of the SF (top) and the isotherms (bottom) for $Dn = 4000$ and $\delta = 0.1$.

Then, we performed the behaviors of the US for $\delta = 0.1$ and $0 < Dn \leq 4000$. Now, we calculate the TEv of λ for $Dn = 100$, where the chaotic flow with 3- vortex solution is observed as shown in Figs. 7(a, c). The chaotic nature has been properly checked by drawing the PS of λ in the $\lambda - \gamma$ plane, where $\gamma = \iint \psi dxdy$.(see Fig. 7(b)), where we observed that the flow is chaotic. With the gradual increase of *Dn*, the chaotic flow turns into the steady-state flow with a 2- vortex solution in Figs. 8(a, b) at $Dn = 500$ and the steady-state flow remained unchanged till $Dn = 4000$. Again, we calculate the time progression of λ at $Dn = 4000$ then we see that the flow is chaotic with 2- to 4-vortex solution as shown in Figs. 9(a, c). For clear observation, we draw a PS of TEv as depicted in Fig. 9(b).

Finally, we evaluated unsteady solutions $\delta = 0.5$. Figs. 10(a, c) suggest the flow is chaotic with a 3- vortex solution $Dn = 100$. For more understanding of the chaoticity, we also assessed the PS of the TEv as exhibited in Figure 10(b) and confirmed chaoticity.

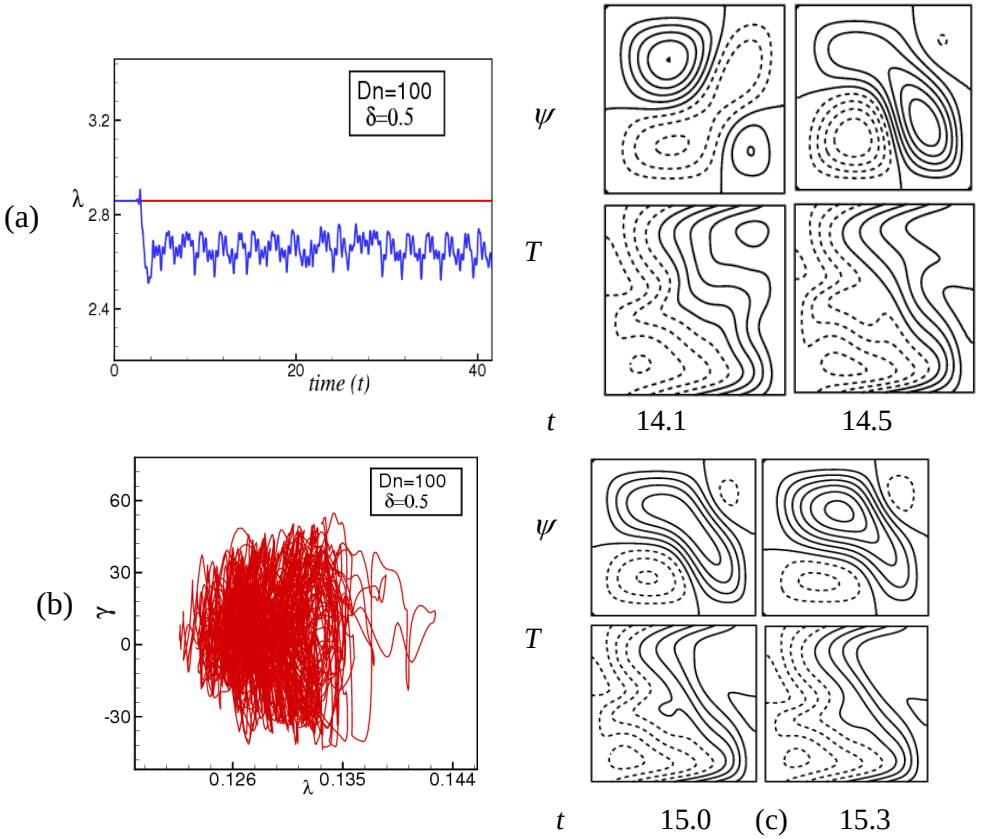

Fig. 10. (a) Time-progression, (b) PS and (c) patterns of the SF (top) and the isotherm (bottom) when $Dn = 100$ and $\delta = 0.5$.

V. Conclusion

A study on numerical and spectral-based has been presented to investigate the characteristics of the flow-through CSD for curvatures ratios 0.001, 0.1, and 0.5 and investigated comprehensively $0 < Dn \le 4000$. We obtained two branches of SSs for each curvature $\delta = 0.001$ and 0.1 while three branches for $\delta = 0.5$ with 2- to 8- vortex solution. We then investigated the US of fluid flows with the calculation of TEv and PS. The UFs undergoes the sequences '*multi-periodic* $\rightarrow$ *steady-state* $\rightarrow$ *chaotic'* for $\delta = 0.001$ and $\delta = 0.1$ while for $\delta = 0.5$, the UF is as follows '*chaotic* $\rightarrow$ *steady-state'*. The typical contour of the patterns of the SF and the isotherms have also been investigated for various *Dn*, where we observed that the UF consists of 2- to 4-vortex solutions. SF plays a vital role in the HT of the fluid from heated wall to neighboring. HT is always enhanced by the chaotic nature than the other physically realizable solutions.

Conflicts of Interest:

The authors declare that they have no conflicts of interest to report regarding the present study.

References

I. Chanda, R. K., Hasan, M. S., Alam, M. M. and Mondal, R. N. (2020), Hydrothermal Behavior of Transient Fluid Flow and Heat Transfer through a Rotating Curved Rectangular Duct with Natural and Forced Convection, *Mathematical Modelling of Engineering Problems*, 7(4), 501-514.

II. H. Ito, Flow in curved pipes, *JSME International Journal*. **30**, 1987, pp.543-52.

III. K. Nandakumar and J. H. Masliyah, Swirling Flow and Heat Transfer in Coiled and Twisted Pipes, *Adv. Transport Process*. **4,** 1986, pp.49-112.

IV. K. Yamamato, W. Xiaoyum, N. Kazou, and H. Yasutuka, Visualization of Taylor-Dean flow in a curved duct of square cross section, *J. Fluid Dyn. Res*. **38**, 2006, pp. 1-18.

V. M. Norouzi, M. H. Kayhani M. R. H. Nobari and M. K. Demneh, Convective Heat Transfer of Viscoelastic Flow in a Curved Duct, *World Academy of Science. Engineering and Technology*. **32**, 2009, pp.327-333.

VI. M. Z. Islam, R. N. Mondal, M. M. Rashidi, Dean-Taylor flow with convective heat transfer through a coiled duct, *Computers and Fluids*. **149**, 2017, pp.41-55.

VII. Md. Hasanuzzaman, Md. Mosharrof Hossain, M.M. Ayub Hossain. : 'SIMILARITY SOLUTION OF HEAT AND MASS TRANSFER FOR LIQUID EVAPORATION ALONG A VERTICAL PLATE COVERED WITH A THIN POROUS LAYER'. *J. Mech. Cont. & Math. Sci., Vol.-16, No.-4, April (2021) pp 47-60*. DOI : https://doi.org/10.26782/jmcms.2021.04.00004

VIII. Rafiuddin, Noushima Humera. G. : ' NUMERICAL SOLUTION OF UNSTEADY TWO - DIMENSIONAL HYDROMAGNETICS FLOW WITH HEAT AND MASS TRANSFER OF CASSON FLUID'. *J. Mech. Cont.& Math. Sci., Vol.-15, No.-9, September (2020) pp 17-30*. DOI : https://doi.org/10.26782/jmcms.2020.09.00002

IX. R. N. Mondal, T. Watanabe, M. A. Hossain and S. Yanase, Vortex-Structure and Unsteady Solutions with Convective Heat Transfer through a Curved Duct, *Journal of Thermophysics and Heat Transfer*. **31**(1), 2017, pp.243-254.

X. R. N. Mondal, Y. Kaga, T. Hyakutake and S. Yanase, Effects of curvature and convective heat transfer in curved square duct flows, *Trans. ASME, Journal of Fluids Engineering*. **128**(9), 2006, pp.1013-1022.

XI. S. A. Berger, L. Talbot, L. S. Yao, Flow in Curved Pipes, *Annual. Rev. Fluid. Mech*. **35**, 1983, pp.461-512.

XII. S. N. Dolon, M. S. Hasan, S. C. Ray, and R. N. Mondal, Vortex-structure of secondary flows with effects of strong curvature on unsteady solutions through a curved rectangular duct of large aspect ratio, *AIP Conference Proceedings*. **2121**, 050004, 2019.

XIII. S. Yanase, Y. Kaga, R. Daikai, Laminar Flows through a curved rectangular duct over a wide range of the aspect ratio, *Fluid Dynamics Research*. **31**, 2002, pp.151–183.

XIV. W. R. Dean, Note on the motion of fluid in a curved pipe, *Philos Mag*. **4**, 1927, pp.208-223.